PROCEEDINGS OF SCIENCE

ONLINE ICRC 2021
THE ASTROPARTICLE PHYSICS CONFERENCE
Berlin | Germany
37th International Cosmic Ray Conference
12–23 July 2021

Characterization of the DIMS system based on astronomical meteor techniques for macroscopic dark matter search

D. Barghini,[a,b,*] S. Valenti,[a] S. Abe,[c] M. Arahori,[d] M. Bertaina,[a] M. Casolino,[e,f] A. Cellino,[b] C. Covault,[g] T. Ebisuzaki,[e] Y. Fujiwara,[h] D. Gardiol,[b] M. Hajdukova,[i] R. Ide,[d] Y. Iwami,[j] F. Kajino,[d] S.-W. Kim,[k] J.N. Matthews,[l] K. Nadamoto,[d] I.H. Park,[m] L.W. Piotrowski,[n] H. Sagawa,[o] K. Shinozaki,[p] D. Shinto,[j] J.S. Sidhu,[g] G. Starkman,[g] S. Tada,[d] Y. Takizawa[e] and Y. Tameda[j] on behalf of the DIMS Collaboration
(a complete list of authors can be found at the end of the proceedings)

E-mail: dario.barghini@edu.unito.it

Nuclearites are strange quark matter conglomerates that are hypothesized as possible candidates of macroscopic dark matter. When impacting the Earth's atmosphere, they should undergo quasi-elastic collisions with the air molecules and emit black-body radiation, thus generating atmospheric luminous events similar to meteors. However, nuclearites could be distinguished from meteors mainly by their altitude, velocity, and motion direction of the bright flight. For instance, nuclearites of galactic origins are expected to have a typical velocity of 250 km s^{-1}, whereas meteors observed in the Earth's atmosphere are bounded to 72 km s^{-1}. In the case of meteoroids of interstellar origin, this value may be exceeded but, considering the stellar velocity distribution in the vicinity of the Sun, only by several kilometres per second. The DIMS (Dark matter and Interstellar Meteoroid Study) experiment was designed to search for such fast-moving particles by observing the sky with wide-field, high-sensitivity CMOS cameras. We derived the calibration of the DIMS sensors by astrometric and photometric techniques applied to observed stars in the field of view and assessed the achieved positional precision and sensitivity levels. Since nuclearites and meteor events feature quite distinct observational conditions, we optimized the DIMS setup and analysis pipeline. The distinct spectrum of mass and velocity of nuclearites must also be taken into account. We consequently evaluated the variability of nuclearites dynamics in the atmosphere in this respect. We also assessed the potentiality of the DIMS system in posing limits for macros observation based on our preliminary results. In this contribution, we will present the current status of this work.

37th International Cosmic Ray Conference (ICRC 2021)
July 12th – 23rd, 2021
Online – Berlin, Germany

*Presenter

PoS(ICRC2021)500

1. Introduction

In the wide range of possible dark matter candidates, the class of macroscopic dark matter is gaining increasing attention in recent years from both experimental and theoretical perspectives. The original idea was proposed by Witten in 1984 [1] who suggested that strange quark matter (SQM), in the form of macroscopic aggregates of up, down and strange quarks, might be more stable than ordinary matter. Later, De Rujula and Glashow [2] developed a theoretical description of the interaction with the Earth's atmosphere of such compact objects, that were named *nuclearites*. They should exhibit a phenomenology similar to meteors but with different signatures, mostly with respect to their typical speed. Up until now and apart from nuclearites, a multitude of models have been proposed following the initial footprints of these ideas, and this broad class of hypothetical dark matter candidates is referred to as *macros* [3].

In this scenario, efforts have been made to provide limits of macros flux, given that such objects should collide with the Earth and produce measurable effects, if they exist. For example, the non-observation of fast-moving bright meteors [4] allowed to rule out certain regions of mass/cross-section for macros observations. Similarly, limits on the flux of nuclearites have been provided by searching for anomalous meteor-like tracks in the data collected by the *Pi of the Sky* experiment [5]. The possibility of detecting nuclearites was also considered by the JEM-EUSO program [6], which included macros investigations in the scientific payload of experiments like Mini-EUSO onboard the International Space Station [7] and future space detectors like POEMMA [8].

The DIMS (Dark matter and Interstellar Meteoroid Study) experiment was born in 2017 aiming to search for fast-moving objects by observing the sky with wide-field and high-sensitivity CMOS cameras [9]. In addition to dark matter investigations, the detection of meteors exceeding the 72 km s^{-1} boundary of meteoroids from the Solar System may give direct evidence of interstellar meteoroids, even though high velocity typically corresponds to lower measurement accuracy due to the shorter measurement time [10]. In this paper, we give a preliminary report on the characterization of the DIMS system designed for macroscopic dark matter search. In Sect. 2 we illustrate the predicted phenomenology of a nuclearite impact onto the Earth's atmosphere, based on current theoretical models. In Sect. 3 we assess the performances of our instruments deduced by astronomical meteor techniques applied to the data from an observational session in 2019. We discuss the potentiality of the DIMS system for macros investigations in Sect. 4 and outline our conclusions in Sect. 5.

2. Nuclearite dynamics in the Earth's atmosphere

The theoretical description given by De Rujula and Glashow [2] considers that a nuclearite, being surrounded by an electron cloud to preserve overall neutrality, should lose energy via quasi-elastic collisions with the molecules of the medium and subsequently forming an expanding thermal cylindrical shock wave, which emits black-body radiation. By considering a nuclearite with nuclear density ($3.6 \cdot 10^{14}$ g cm^{-3}), the luminous efficiency is estimated to be about 4% and independent from both mass and velocity of the object. It is also assumed that nuclearites collides with the atmosphere with a velocity of 250 km s^{-1}, that is the typical rotation speed of the Galaxy and does not consider the Earth motion. Since it has been suggested that such objects may have velocities up to 550 km s^{-1}, *i.e*, the escape limit from the Galaxy at the Sun's position, we provide here a

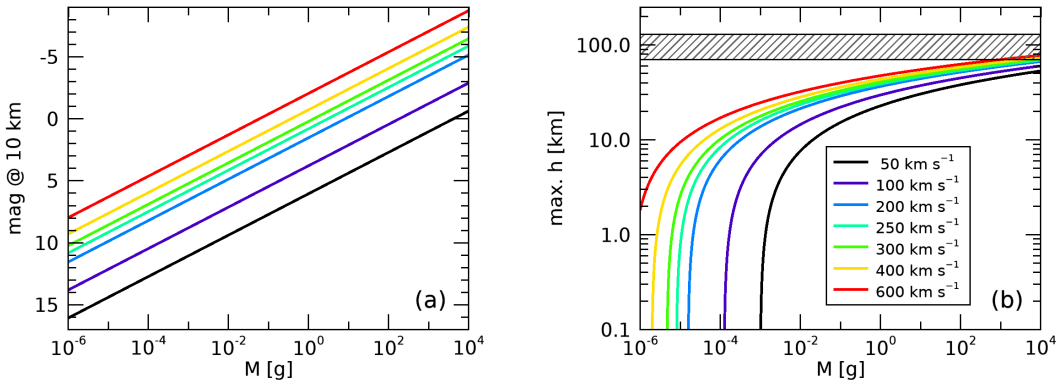

Figure 1: Visual magnitude at 10 km of altitude (a) and maximum height of light emission (b) as a function of the nuclearite mass, for different velocities within 50 and 600 km s^{-1}, according to Eqs. 1 and 2. The grey dashed region in panel (b) marks the altitude range in which meteors typically occur (from 70 to 130 km).

generalization of the expression from [2] of the nuclearite visual magnitude $\mathcal{M}$ as:

$$\mathcal{M} = 0.80 - 1.67 \log_{10}\left(\frac{M}{1\ \mathrm{g}}\right) + 5 \log_{10}\left(\frac{h}{10\ \mathrm{km}}\right) - 7.5 \log_{10}\left(\frac{v}{250\ \mathrm{km\ s^{-1}}}\right) , \tag{1}$$

where M and v are the nuclearite mass and velocity, and h is its altitude from ground. We can also compute the maximal height at which a nuclearite is supposed to generate light as:

$$\frac{h_{max}}{1\ \mathrm{km}} = 3.3 \left[\ln\left(\frac{M}{1\ \mathrm{g}}\right) + 3 \ln\left(\frac{v}{250\ \mathrm{km\ s^{-1}}}\right)\right] + 38.79 . \tag{2}$$

Figure 1 plots the visual magnitude at 10 km of altitude (a) and the maximum height of light emission (b) as a function of the nuclearite mass and for different velocities, from 50 to 600 km s^{-1}. Since the object becomes brighter as its velocity increases, nuclearites moving at $v > 400$ km s^{-1} would be detectable by DIMS cameras even with a mass of 0.1 mg, close to the local dark matter flux limit [2]. The grey dashed region plotted in Fig. 1b marks the altitude range in which meteors typically occur, from 70 to 130 km. Then, nuclearites should emit light at a lower altitude (typically < 60 km) with respect to meteors, and only massive nuclearites with $v > 600$ km s^{-1} (beyond the escape limit from the Galaxy) would start to shine within the meteor region. Consequently, the event altitude is a useful parameter to discern between nuclearites and meteors phenomenology and should be considered together with the observed speed, which however for a nuclearite might happen to be in the allowed range for Solar System's meteors.

A different model was proposed in recent years [11] to describe the macro's phenomenology traversing the atmosphere. In this case, the macro is considered as a point-like source travelling along a straight line and creating a hot plasma channel, which expands by heat diffusion. The plasma channel reaches a maximum section and extinguishes within a cooling time, given by the velocity, cross-section and altitude of the macro. Considering that the plasma should be optically thin (except only for very massive macros), the luminous efficiency is computed from the plasma recombination rate. According to this model, the expected visual magnitude can be given as:

$$\mathcal{M} = 39.66 - 5 \log_{10}\left(\frac{M}{1\ \mathrm{g}}\right) + 5 \log_{10}\left(\frac{h}{10\ \mathrm{km}}\right) + 5 \log_{10}\left(\frac{\rho_N}{\rho}\right) + \frac{1}{\ln 10}\left(\frac{h}{1\ \mathrm{km}}\right) . \tag{3}$$

Then, a macro of $M = 1$ g, with a nuclear density $\rho = \rho_N$ and at an altitude $h = 10$ km would have a visual magnitude of $\mathcal{M} = +44$. Instead, Eq. 1 for $v = 250$ km s^{-1} gives $\mathcal{M} = +0.8$. A similar comparison carried out for macro detection at space-based and suborbital experiments of JEM-EUSO is presented in [12]. The difference $\Delta\mathcal{M} \sim +43$ between the two values is abysmal and points out that, according to [11], a macro of 1 g mass and nuclear density would produce a signal way too dim to be detected by any kind of ground-based detector.

3. Data analysis

The DIMS experiment was designed with the main focus on the investigation of macros and interstellar meteoroids flux at the Earth. A description of the project and first preliminary results are given in [9]. In this work, we will focus on the analysis of the data taken during the night of 1st September 2019 at the Telescope Array (TA) site, in Utah, with two Canon ME20F-SH monochrome cameras, equipped with Canon EF35mm f/1.4L lenses and a 1920×1080 pixels CMOS sensor and operated at a 29.97 Hz frame rate. The trigger and acquisition software used was UFOCapture[1], designed for meteor observation. The cameras, named N1 and N2, were installed at the Hinckley and Black Rock Mesa sites, respectively, at a distance of about 17 km and pointing towards Polaris. The two cameras observed continuously the sky for 6.5 hours and triggered about 400 events in coincidence between the two.

3.1 Astrometric calibration

Since triggered videos with meteors usually last few seconds, the astrometric calibration of the focal plane is performed over a median frame by means of positions of observed stars in the field of view (FoV). We use the Hipparcos-Tycho catalogues [13, 14] as a reference for both astrometric and photometric calibrations. The implemented approach is similar to the one developed for the calibration of the all-sky cameras of the PRISMA fireball network [15]. A search and centring of bright sources is performed via marginal distribution fitting, providing a list of positions (x, y) onto the focal plane. Then, catalog equatorial positions (α_c, δ_c) are correlated to (x, y) via a first simple polar projection. To fit a refined astrometric solution, we choose a standard CD matrix approach, accounting for plate rotation and scaling, plus an 8th degree TNX[2] complete polynomial distortion. This process is iteratively repeated, by each step searching for fainter sources, increasing the magnitude limit on the catalogue and refining the plate solution.

Figure 2 displays the results of the astrometric and photometric calibrations on a sample event from N1 camera captured at 08:16:17 UT. A portion of the FoV around the meteor is pictured in Fig. 2a, together with the found sources, circled in red, which were associated with a catalogue entry. The total FoV of our cameras results to be about $57^\circ \times 34^\circ$ with a pixel linear angular aperture of approximately $1.8'$. By imposing a limit magnitude of +8 on the catalogue, we are able to automatically identify about 900 stars per image. Figure 2b and c plot the equatorial coordinate residuals for the deduced plate solution. No systematic is evident, and residuals are shown to be normally distributed around zero with a standard deviation of about $0.25'$ (~ 0.15 px) for both right ascension and declination, showing that we are achieving a sub-pixel positional precision.

[1] https://sonotaco.com/soft
[2] https://fits.gsfc.nasa.gov/registry/tnx.html

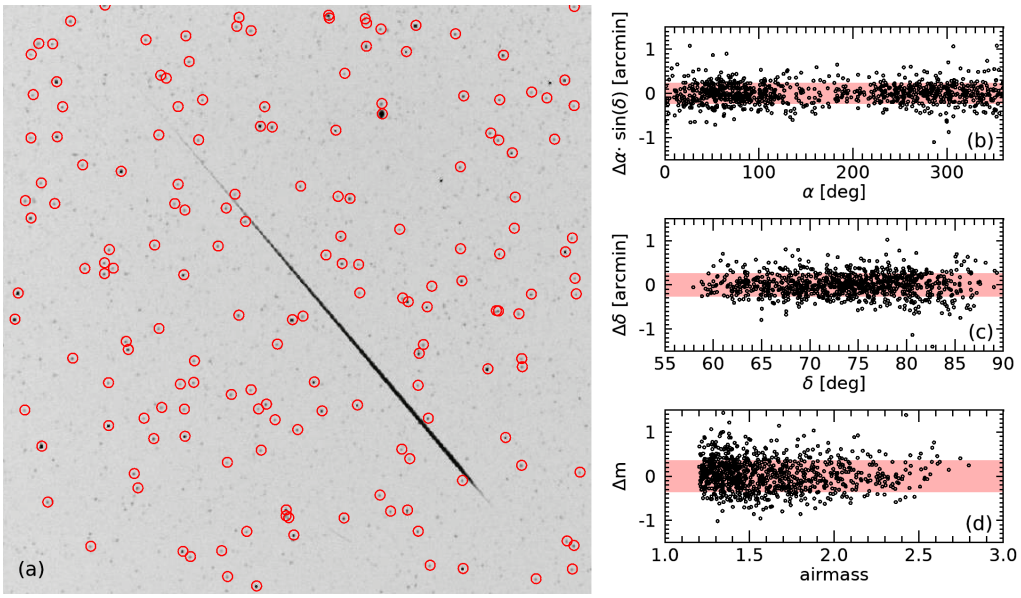

Figure 2: Calibration results on a sample event captured from N1 camera at the Hinckley TA site on the 1st September 2019 at 08:16:17 UT. (a) A portion of the FoV (with inverted colour scale) with the track of the triggered meteor together with positions identified stars, as red circles, up to +8 mag; (b) right ascension residuals between calibrated and catalogued stars positions; (c) same as panel b, but for declination; (d) magnitude residuals as a function of the airmass.

3.2 Photometric calibration

DIMS cameras were calibrated with a large integrating sphere at the National Institute of Polar Research[3]. These measurements allow us to correct for the efficiency lowering from the centre to the edges of the focal surface. According to the approach proposed in [16], the relative efficiency η can be empirically modelled as a function of the radial distance r from the FoV centre as:

$$\eta(R) = 1 - A_0 r - A_1 \left[e^{-\frac{A_0}{A_1} r} - 1 \right] , \tag{4}$$

which fulfils the operative requirements of $\eta(0) = 1$ and $\eta'(0) = 0$. From our measurements, we estimate $A_0 = (750 \pm 4) \cdot 10^{-6}$ px^{-1} and $A_1 = (97 \pm 3) \cdot 10^{-3}$. The relative efficiency drops with an asymptotic linear loss of about 7.5% each 100 px, and reaches as low as 30% to the very edge of the focal surface ($r \sim 1110$ px).

Our system has a wide bandpass, given by the quantum efficiency of the CMOS sensor which roughly covers the range from 0.3 to 1 µm, is centred at 0.5 µm and has a full width at half maximum of about 0.4 µm. According to these specifications, we choose the Hipparcos magnitude H_p as the reference magnitude for the photometric calibration. Figure 2d plots the magnitude residuals (between catalogued and experimental values) as a function of the airmass for the sample event, showing a standard deviation of about 0.35 mag. From our analysis, we cannot recognize any evident dimming for increasing airmass, so that we neglect the effect of differential atmospheric extinction in this calibration.

[3] http://polaris.nipr.ac.jp/~uap/IntegrationSphere/

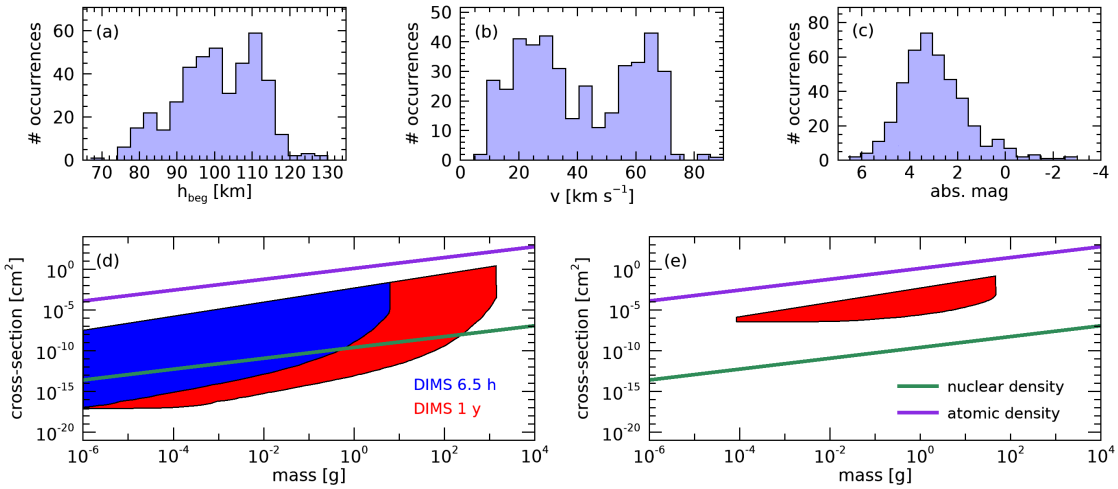

Figure 3: Statistics of main meteor physical parameters from the DIMS dataset presented in this work and expected macro's constraints. (a) Distribution of meteor beginning height; (b) velocity; (c) absolute magnitude; (d) constraints by DIMS for 6.5 hours exposure of the current dataset (blue area) and for 1-year projection with 10% duty cycle (red area), according to [2]; (e) same as panel d, according to [11]. The green and purple line in panels d,e plots the cross-section respectively for macros with nuclear and atomic density.

4. Expected macros constraints by the DIMS experiment

The results of the calibration process of each video are therefore used to derive the equatorial positions and magnitude of the captured event. Then, triangulation between N1 and N2 cameras provides the three-dimensional trajectory of the event in the atmosphere, in the straight-line hypothesis [17]. Figure 3a-c shows the statistics of the main physical parameters deduced from this analysis applied to the dataset presented in this paper. The beginning heights (Fig. 3a) are distributed between 70 and 130 km, as expected for typical meteors. The entry velocity histogram (Fig. 3b) presents the typical bi-variated distribution for low (asteroidal) and high (cometary) velocity. Only 8 events show a median speed above the 72 km s^{-1}, but they can be ruled out since they were found to be badly reconstructed from triangulation. The absolute magnitude distribution of Fig. 3c, corresponding to a 100 km reference altitude for meteors, suggests that the DIMS system is not completely efficient in detecting meteors fainter than absolute magnitude +4 mag. The limiting value of absolute magnitude for meteors turns out to be about +6. None of the analyzed events shows indisputable features indicating non-meteor origin.

Therefore, we evaluate the expected constraints to macros flux that could be established thanks to the DIMS experiment, following the approach proposed in [4] and considering the DIMS limiting magnitude and FoV discussed above. Not having observed any anomalous event in our dataset, this would allow to rule out a certain region in the macro parameters space of mass and cross-section. The boundary of this region depends upon which model we consider for the macro phenomenology (Sect. 2). Figure 3d plots this region, according to [2], for the exposure time of the 1st September 2019 night (6.5 hours, blue area) and the expected limits for 1 year of DIMS observations by assuming a 10% duty cycle (red area). In this scenario, DIMS would be able to probe macros with nuclear density (green line) and masses up to $\sim$ 10 g with the data from this night and has

the potentiality to reach $\sim 10^3$ g in the 1-year projection. This result is drastically different if we consider the model by [11]. From Fig. 3e, it turns out that DIMS cannot rule out any region in the parameter space with the dataset presented in this paper and would reach masses up to $\sim 10^2$ g in the 1-year projection, however not being able to probe macros with nuclear density.

5. Conclusions

We presented in this work a preliminary report on the characterization and the potentiality of the DIMS experiment for macroscopic dark matter search. We reviewed two theoretical models [2, 11] for the interaction of such compact objects into the Earth's atmosphere and provided a generalization for the expected velocity range for the first one. The difference between the visual magnitude from the two models is abysmal and can be resolved only by considering very massive objects or below the nuclear density. We illustrated the performances of our sensors deduced from the astrometric and photometric calibration over the observed stars in the FoV of the camera. With the current setup, the DIMS limiting absolute magnitude for meteors observation is found to be about +6. From triangulation between N1 and N2 cameras, we deduced the main physical parameters and presented their statistics for the 6.5 hours acquisition night on 1st September 2019. None of the analyzed events clearly pointed out a non-meteor origin. We therefore assessed the potentiality of DIMS in ruling out a part of parameters space of macros, according to the two theoretical models. We presented here the best constraints under the assumption of a 100% efficiency at the limiting magnitude +6, but we know that this is not realistic above +4 mag. The estimation of the real efficiency for faint magnitudes will require extensive simulations that are part of the future work. Further investigations will address the efficiency of the current DIMS trigger in detecting very fast events, which is crucial for our considerations, and the design of a dedicated trigger in this respect.

Acknowledgments

This work is partially supported by JSPS KAKENHI Grant Number JP19H01910, by the joint research program of the Institute for Cosmic Ray Research (ICRR), the University of Tokyo, and by National Science Centre, Poland grant 2020/37/B/ST9/01821. We thanks to members of Telescope Array experiment for their help to achieve the observations. The authors from the University of Turin acknowledge support from Compagnia di San Paolo within the project ex-post-2018.

References

[1] E. Witten, *Cosmic separation of phases*, *Phys. Rev. D* **30** (1984) 272.

[2] A. De Rujula and S.L. Glashow, *Nuclearites-a novel form of cosmic radiation*, *Nature* **312** (1984) 734.

[3] D.M. Jacobs et al., *Macro dark matter*, *Mon. Not. R. Astron. Soc.* **450** (2015) 3418.

[4] J.S. Sidhu and G. Starkman, *Macroscopic dark matter constraints from bolide camera networks*, *Phys. Rev. D* **100** (2019) 123008.

[5] L.W. Piotrowski et al., *Limits on the Flux of Nuclearites and Other Heavy Compact Objects from the Pi of the Sky Project*, *Phys. Rev. Lett.* **125** (2020) 091101.

[6] J.H. Adams et al., *JEM-EUSO: Meteor and nuclearite observations*, *Exp. Astron.* **40** (2015) 253.

[7] S. Bacholle et al., *Mini-EUSO Mission to Study Earth UV Emissions on board the ISS*, *Astrophys. J.,Suppl. Ser.* **253** (2021) 36.

[8] Poemma Collaboration, A.V. Olinto et al., *The POEMMA (Probe of Extreme Multi-Messenger Astrophysics) observatory*, *J. Cosmol. Astropart. Phys.* **2021** (2021) 007.

[9] F. Kajino et al., *Study for Moving Nuclearites and Interstellar Meteoroids using High Sensitivity CMOS Camera*, in *36th ICRC - 2019*, vol. 36 of *International Cosmic Ray Conference*, p. 525, July, 2019.

[10] M. Hajdukova et al., *The challenge of identifying interstellar meteors*, *Planet. Space Sci.* **192** (2020) 105060.

[11] J.S. Sidhu et al., *Macro detection using fluorescence detectors*, *J. Cosmol. Astropart. Phys.* **2019** (2019) 037.

[12] L.A. Anchordoqui et al., *Prospects for macroscopic dark matter detection at space-based and suborbital experiments*, *arXiv e-prints* (2021) arXiv:2104.05131 [2104.05131].

[13] M.A.C. Perryman et al., *The HIPPARCOS Catalogue*, *Astron. Astrophys.* **323** (1997) L49.

[14] E. Høg et al., *The TYCHO Catalogue*, *Astron. Astrophys.* **323** (1997) L57.

[15] D. Barghini et al., *Astrometric calibration for all-sky cameras revisited*, *Astron. Astrophys.* **626** (2019) A105.

[16] D. Barghini et al., *Improving astrometry and photometry reduction for PRISMA all-sky cameras*, in *Proc. 37th IMC Pezinok-Modra, 2018*, R. Rudawska et al., eds., pp. 41–45, 2019.

[17] J. Borovička, *The Comparison of Two Methods of Determining Meteor Trajectories from Photographs*, *Bull. Astron. Inst. Czech.* **41** (1990) 391.

Affiliations

[a] *Department of Physics, University of Turin, Italy*
[b] *Astrophysical Observatory of Turin, National Institute for Astrophysics (INAF), Italy*
[c] *Department of Aerospace Engineering, Nihon University, Japan*
[d] *Department of Physics, Konan University, Japan*
[e] *RIKEN (Institute of Physical and Chemical Research), Japan*
[f] *National Institute for Nuclear Physics (INFN) - Rome Tor Vergata, Italy*
[g] *Department of Physics, Case Western Reserve University, USA*
[h] *Nippon Meteor Society (NMS), Japan*
[i] *Astronomical Institute of Slovak Academy of Sciences, Slovakia*
[j] *Department of Engineering and Science, Osaka Electro-Communication University (OECU), Japan*
[k] *Korea Astronomy and Space Science Institute (KASI), Republic of Korea*
[l] *Department of Physics and Astronomy, University of Utah, USA*
[m] *Department of Physics, Sungkyunkwan University, Republic of Korea*
[n] *Faculty of Physics, University of Warsaw, Poland*
[o] *Institute for Cosmic Ray Research, University of Tokyo, Japan*
[p] *National Centre for Nuclear Research (NCBJ), Poland*

Full Authors List: DIMS Collaboration

S. Abe.[1], M. Arahori[2], D. Barghini[3,6], M. Bertaina[3], M. Casolino[4,5], A. Cellino[6], C. Covault[17], T. Ebisuzaki[4], M. Endo[1], M. Fujioka[9], Y. Fujiwara[7], D. Gardiol[6], M. Hajdukova[8], M. Hasegawa[1], R. Ide[2], Y. Iwami[9], F. Kajino[2], M. Kasztelan[16], K. Kikuchi[1], S.-W. Kim[10], M. Kojro[11], J.N. Matthews[12], K. Nadamoto[2], I.H. Park[13], L.W. Piotrowski[14], H. Sagawa[15], K. Shinozaki[16], D. Shinto[9], J.S. Sidhu[17], G. Starkman[17], S. Tada[2], Y. Takizawa[4], Y. Tameda[9], S. Valenti[3], and M. Vrabel[16]

[1]Department of Aerospace Engineering, Nihon University, Japan
[2]Department of Physics, Konan University, Japan
[3]Department of Physics, University of Turin, Italy
[4]RIKEN (Institute of Physical and Chemical Research), Japan
[5]National Institute for Nuclear Physics (INFN) - Rome Tor Vergata, Italy
[6]Astrophysical Observatory of Turin, National Institute for Astrophysics (INAF), Italy
[7]Nippon Meteor Society (NMS), Japan
[8]Astronomical Institute of Slovak Academy of Sciences, Slovakia
[9]Department of Engineering and Science, Osaka Electro-Communication University (OECU), Japan
[10]Korea Astronomy and Space Science Institute (KASI), Republic of Korea
[11]Faculty of Physics and Applied Informatics, University of Lodz, Poland
[12]Department of Physics and Astronomy, University of Utah, USA
[13]Department of Physics, Sungkyunkwan University, Republic of Korea
[14]Faculty of Physics, University of Warsaw, Poland
[15]Institute for Cosmic Ray Research, University of Tokyo, Japan
[16]National Centre for Nuclear Research (NCBJ), Poland
[17]Department of Physics, Case Western Reserve University, USA

PoS(ICRC2021)500